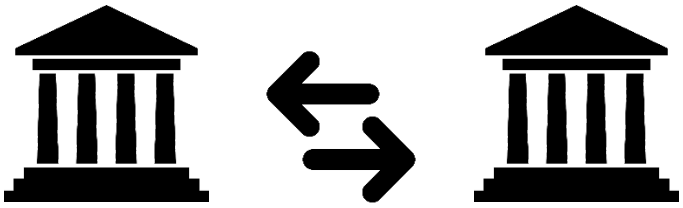

This PDF has been sent from one of the University of Delaware's partner libraries through Interlibrary Loan. It will be in your account for **30 days**. After 30 days, the PDF will be permanently deleted.

If you received the wrong item, or if there are any other problems with the PDF (such as missing pages or unclear images), **please contact the Interlibrary Loan Office**. We will ask the supplier for a corrected copy.

Interlibrary Loan Office
AskILL@udel.libanswers.com

UNIVERSITY OF DELAWARE
LIBRARY, MUSEUMS
& PRESS

Science of the Total Environment 792 (2021) 148353

Contents lists available at ScienceDirect

Science of the Total Environment

journal homepage: www.elsevier.com/locate/scitotenv

Tracing the sources of phosphorus along the salinity gradient in a coastal estuary using multi-isotope proxies

Qiang Li [a], Hezhong Yuan [a,b], Hui Li [a], Christopher Main [c], Jessica Anton [a], Deb P. Jaisi [a,*]

[a] Department of Plant and Soil Sciences, University of Delaware, Newark, DE 19716, United States
[b] School of Environmental Science and Engineering, Nanjing University of Information Science & Technology, Nanjing, Jiangsu 210044, PR China
[c] Department of Natural Resources and Environmental Control, Dover, DE 19901, United States

HIGHLIGHTS

- Different sources of colloids have different P pools and isotopes of C, N, and PO_4.
- Major source of P in Love Creek switches from non-tidal to tidal stretch of the creek.
- Season and tidal cycle complicate the accurate assessment of sources.

GRAPHICAL ABSTRACT

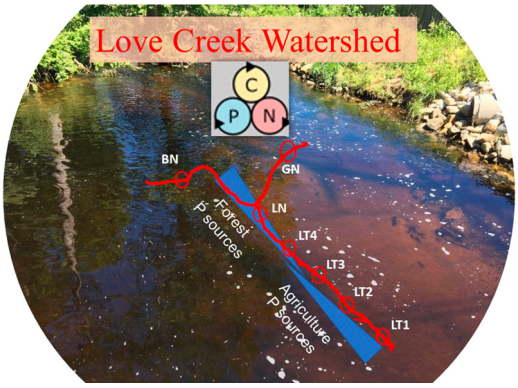

ARTICLE INFO

Article history:
Received 19 March 2021
Received in revised form 1 June 2021
Accepted 5 June 2021
Available online 8 June 2021

Keywords:
Love Creek watershed
Phosphorus
Source tracking
Isotopes
Tidal and non-tidal water

ABSTRACT

Eutrophication in coastal water has compromised ecosystem services. Identification of phosphorus (P) sources and their load contributions are required for the development of effective nutrient management plans. In this research, multi-isotope proxies were applied to track P sources and evaluate their relative contributions in Love Creek, a coastal estuary in Delaware. The isotope values of carbon (*ca.* −22‰), nitrogen (*ca.*+6‰), and phosphate oxygen (*ca.*+18‰) of agricultural soils under different agricultural practices are generally similar even though their concentrations are distinctly different from forest soils ($\delta^{13}C$: *ca.* −27‰; $\delta^{13}N$: *ca.*+2‰; $\delta^{18}O_P$: *ca.*+22‰). Comparison of these parameters among potential land sources (agricultural soils, forest soils, septic wastes, and plant debris) and sink (colloids in water) revealed that the plant debris and soils from forest sources are likely dominant sources of P in freshwater sites. The contribution of terrestrial P sources gradually decreased along the salinity gradient and agricultural soil sources gradually dominanted in the saline water portion of the creek. The variations of P loads due to weather-related discharge, changing land use and activities, and seasons were high and reflected the limitation of accurate estimation of sources. Overall, these results provide improved insights into potential sources and biogeochemical processes in the estuary, which are expected to be useful for water quality monitoring programs.

1. Introduction

Phosphorus (P) contamination in coastal waters worldwide has compromised ecosystem benefits by decreasing the values of natural goods and services and reducing incomes from tourism and recreational

* Corresponding author.
E-mail address: jaisi@udel.edu (D.P. Jaisi).

https://doi.org/10.1016/j.scitotenv.2021.148353
0048-9697/

activities. Federal, state, local, and private agencies actively seek solutions to minimize nutrient-related water quality reduction. Still, the success has been limited primarily due to the limited understanding of specific sources that cause to deteriorate the water quality. It means the identification of nutrient load contributions from different sources is required to develop an effective management plan and to reduce nutrient loads. Further, spatial and temporal variations in sources, flux, and variable transformation among their forms, complicate the understanding of the sources and processes. These limitations point toward the need for the tracers in source tracking and biogeochemical cycling research.

Oxygen isotope composition of phosphate ($\delta^{18}O_P$) have been increasingly used as a reliable tool to trace P sources in a variety of ecosystems such as agricultural, freshwater, and marine ecosystems (Angert et al., 2012; Bauke et al., 2018; Bi et al., 2018; Davies et al., 2014; Gooddy et al., 2016; Joshi et al., 2016; Hacker et al., 2019; Tamburini et al., 2012; Siebers et al., 2018; Tonderski et al., 2017). The fundamentally distinct properties of $\delta^{18}O_P$ value in biotic and abiotic sources enable it to serve as a tracer to identify P cycling and transformation in complex ecosystems. Regardless, slight variations in the isotopic signature of P from multiple sources and overprinting of the signatures during P transformation in soils and waters complicate the accurate identification of sources (Gross and Angert, 2015; Joshi et al., 2016; Granger et al., 2017). However, coupling $\delta^{18}O_P$ values with other reliable stable isotopic tools, including carbon (C) and nitrogen (N), provide a complementary and independent proxy to identify sources.

Losses of colloidal and dissolved P from soils can occur along surface and subsurface pathways (McDonnell et al., 2010; Sharpley et al., 2015), at various proportions and the transported P may conserve isotope signal from its source. The correct interpretation of oxygen isotope values in phosphate requires understanding of related processes and reactions that may alter primary isotopic compositions as well as physical processes such as transport and mixing. Similarly, C isotopes has been successfully applied to track the origin of soil organic matter (SOM) across soil profile *via* characterization of C isotopic signatures of different soil size fractions (Desjardins et al., 1994). However, soils are almost always considered as whole in isotope research without considering different size fractions, which could have different isotope signatures. Further, erosion preferentially removes finer-sized particles, which are enriched in P than coarser-sized particles. Pedological processes and microbial activities in the different size fractions are expected to be different. These characteristics necessitate the analysis of different size fractions at source sites for a fuller understanding of their contribution to sinks. To better account for these variabilities, a relatively smaller watershed with a limited number of potential P sources is ideal for testing hypotheses on the role of different variables.

Love Creek, located upstream of Rehoboth Bay, is a small tributary of Delaware Inland Bays and is designated as the water of exceptional recreational of ecological significance (ERES) by the state because of the extensive recreational usage of the water at its mouth. It means the environmental health of the watershed could benefit substantially from improved knowledge in identifying nutrient sources polluting the beach waters. Therefore, the objectives of this research are twofold: 1) determine isotopic signatures of different sources including different particle sizes of soils that are prone to erosion and 2) compare the muti-isotope proxies of sources and sinks to identify P loading in the Love Creek watershed.

2. Study area, materials, and methods

2.1. Study area

Love Creek is a coastal tidal estuary located in the eastern part of Delaware and upstream of Rehoboth Bay (Figs. 1 and SI1), which drains into the Atlantic Ocean. The upstream portion of the creek is freshwater and covers about 45% of the watershed of approximately 62 km^2. It is surrounded primarily by agricultural farms interspersed with small patches of forest and a few residential areas. The tidal portion of the creek extends upstream to the dam at Goslee Pond at Route 277 (Robinsonville Road). The Downstream of the dam shows a strong salinity gradient, which steadily increases toward the mouth in Rehoboth Bay.

Love Creek watershed has undergone significant changes in land use in recent decades. An increase in land development for housing and recreational purposes is reflected in the high density of septic tank systems in residential areas near the creek (Fig. SI1). Relatively sand-rich soil in the upstream watershed creates an ideal condition for groundwater recharge. Further, a mildly elevated topography in the watershed constitutes a higher groundwater discharge potential to the creek.

2.2. Collection of soil, septic waste, leaf litter, and water

Based on the land use and development in the watershed, potential terrestrial P sources that might potentially reach the creek include soils from agricultural and forest lands, tree and leaf litters from forests, and septic wastes. The isotopic signatures of any particular land use can vary

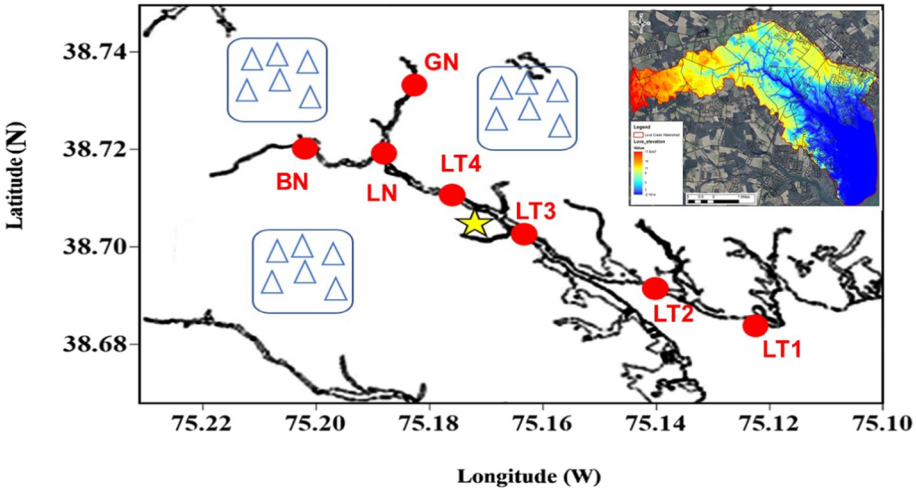

Fig. 1. Sampling sites in the Love Creek watershed: blue triangles within rectangles indicate soil sampling sites; red circles denote water sampling sites (GN, BN, LN, LT4, LT3, LT2 and LT1), and yellow star represents the septic tank collection site . The elevation map of the watershed is included in the inset (*see* Fig. SI1) (DCIB, 2018). The locations of septic tank and soil sampling sites in the map are arbitrary and are not accurate. (For interpretation of the references to color in this figure legend, the reader is referred to the web version of this article.)

based on the length and intensity of the cropping system and fertilization history. To account these variabilities, multiple sampling sites were chosen from each land use type based on i) P concentration, a potential hotspot for P loss; ii) land elevation, a geomorphic feature that determines the extent of soil erosion; iii) soil type, organic content and other elemental and mineralogical compositions that affect nutrient cycling; and iv) regions with high groundwater discharge potential for subsurface transport of P. Agricultural soils were collected from multiple sites based on the crop type, nutrient content, and agricultural practice such as tilling and no-tilling because tilling loosens the soil aggregates and facilitates erosion. Soils from the forest as well as leaf litters adjacent to the creek were also collected. Most soil sampling sites were selected to be proximal to Love Creek including rivulets and brooks that discharge into the creek. To obtain representative soils prone to erosion as well as to identify any changes in isotopic signatures of soil size fractions along with soil depth, topsoil (0 to 10 cm depth) was collected from three farms (from LC1 to LC19) located on the headwaters and middle section of Love Creek. Among the 19 sites chosen, LC16 and LC19 are from fallow soils, which did not receive fertilizers for the past several years and all other soils (LC1–5; LC8–12; LC13–19) are from farms with active fertilizer application and cropped soybean and corn. To identify the nutrient composition in agronomically relevant depth, surface and subsurface (10 to 20 cm) soils were collected from sites LC9, LC10, LC11, and LC17. The forest soils (LC6, LC7) were collected from the representative forest patches in the headwaters of the Love Creek watershed. In each sampling site, five subsamples were collected and thoroughly mixed to form one composite soil sample per site.

Site selection for sewage waste from septic systems was limited due to accessibility to private septic tanks, so are not fully representative of neighborhoods in the watershed. As shown in Fig. SI1, septic tank density is high in the middle stretch of the watershed and region surrounding the Rehoboth Bay. Septic tank density larger than four units per acre and within 100 m from water bodies is considered to impact water quality (NESM, 1973). Therefore, areas with high septic density and within a 100 m proximity to Love Creek were selected for sampling. Upon the landowners' approval, septic tank wastes (6 L, in duplicate) were collected and chilled immediately on the ice during transportation and then stored at 4 °C before processing.

Being a coastal estuary, Love Creek is influenced by the tidal effect of the Inland Bays. To represent both the tidal and non-tidal portions of the creek, seven sites were selected for collecting water samples across a salinity gradient (Fig. 1). Those sites include Bundicks non-tidal 1 (BN), Goslee non-tidal 1 (GN), Love non-tidal 1 (LN), Love tidal 1 (LT1), Love tidal 2 (LT2), Love tidal 3 (LT3), and Love tidal 4 (LT4). Sites BN and GN are located at Bundicks Branch and Goslee Millpond, respectively, which are two small tributaries at the upstream of the creek. Because of the high density of septic systems and agricultural land in the headwater, nutrient loads from these tributaries are expected to be high. Based on preliminary data on P concentrations, 48 to 56 L of water from each site was collected during baseflow conditions over a period of six months. All waters were collected carefully during ebb tide without any disturbance that might cause resuspension of the bottom sediment. Collected water samples were chilled on ice immediately after collection and during transportation and then stored at 4 °C before processing.

Colloids in the creek water samples were separated into three size ranges: a) ≥53 μm, b) 0.45–53 μm, and c) 0.10–0.45 μm, based on the Stokes' law of settling using centrifugation (Sorvall LYNX 6000, Thermo). Prior to separation, visible plant debris and algae filaments were removed carefully using pipettes. The supernatant was decanted and pelleted colloids were freeze-dried. Since the salinity of non-tidal sites was <1.0 practical salinity unit (PSU), no washing or salinity correction was needed to obtain the accurate mass of colloids. For tidal sites, colloids were washed three times to remove salts, which were confirmed by the absence of visible white salt precipitates in freeze-dried colloids. Water temperature, dissolved oxygen concentrations, turbidity, and salinity were recorded on-site at the time of sample collection. Other water parameters were characterized either by the Environmental Laboratory at the Department of Natural Resources and Environmental Control (DNREC) (Main et al., 2020) or University of Delaware.

2.3. Size separation of soil

All collected soils were stored at −12 °C and freeze-dried. Dry samples were dissolved in water (1:10 mass: volume) and <53 μm size fraction was separated by wet sieving. This size fraction was further diluted to make a 1% (1:100 m:v) suspension and centrifuged to separate into two sizes, <0.1 and <0.45 μm size fractions, similar to colloids in the creek (see below). Because of the low mass of 0.10 to 0.45 μm size fractions in soils, freeze-dried samples from the same farm (LC1–5; LC8–12; LC13–18) and land use (LC6–7; LC16–19) were combined. For each soil fraction, isotopes of carbon, nitrogen, and phosphate oxygen were measured.

2.4. Characterization of soil, colloids, and plant debris

Revised sequential extraction method (Hedley and Stewart, 1982) per Joshi et al. (2016) was used to differentiate and quantify different P pools (H_2O-P_i, $NaHCO_3$-P_i, NaOH-P_i, and HNO_3-P_i) in soils and colloids in the creek water. The revisions include steps to recover extracted P adsorbed onto the residual solid phase: 0.5 mol/L $NaHCO_3$ extraction and H_2O rinse were added after the NaOH and HNO_3 extractions. The concentration of P_i in each pool was measured using the phosphomolybdate blue method (Murphy and Riley, 1962). For all soils and colloids, the solid: solution ratio and other extraction conditions (time, temperature, shaking speed) were kept constant, while plant debris was treated differently following the Pfahler et al. (2013) method. Plant debris was oven-dried at 65 °C, ground, and then treated with 0.3 M trichloroacetic acid (TCA) (Hawkins and Polglase, 2000) to extract the TCA-soluble reactive P (TCA-P). This pool is considered rapidly cycling P in plant cells. The residual plant material was subsequently extracted with 10 M nitric acid for total P (Pfahler et al., 2013). The concentrations of P and other elements in both extractions were measured by using inductively coupled plasma optical emission spectrometry (ICP-OES).

2.5. Measurement of C and N isotopes

Approximately 10 mg of freeze-dried and size-fractionated soils, colloids, and plant debris were used to measure carbon isotopes ($\delta^{13}C$) and nitrogen isotopes ($\delta^{15}N$) using an Elemental Analyzer (EA) (Costech, CA, USA) connected with a Delta V IRMS (ThermoFisher Scientific, Germany). All $\delta^{13}C$ and $\delta^{15}N$ values were calibrated against two USGS isotope standards: USGS40 ($\delta^{13}C = -26.39‰$ and $\delta^{15}N = -4.52‰$) and USGS41 ($\delta^{13}C = +37.63‰$ and $\delta^{15}N = +47.57‰$). All measured N and C isotope values are reported in standard delta notation in per mil (‰) unit with respect to atmospheric air and Pee Dee Belemnite (VPDB), respectively.

2.6. Purification of P pools and measurement of oxygen isotopes of water and phosphate

Sequentially extracted P pools were further processed to remove contaminants and concentrate P_i before the precipitation of silver phosphate (Ag_3PO_4) following the method described in Joshi et al. (2018). All extracted solutions were first treated with nonionic, microporous DAX 8 Superlite resin to remove the bulk of the dissolved organic matter. The clear solution produced was further processed to reduce the volume and concentrate the P_i by the Mg-induced co-precipitation (MagIC) method (Karl and Tien, 1992). MagIC pellets were dissolved and then evaporated to attain a final P_i concentration of ≥500 μM before

ammonium phosphomolybdate (APM) precipitation. APM precipitation at low pH allowed removal of contaminants that are acid-soluble, while the following stage of magnesium ammonium phosphate (MAP) precipitation at high pH eliminated alkali-soluble contaminants. The MAP crystals were then dissolved, pH neutralized, and further treated with a cation resin to remove cations. Silver amine solution was used to precipitate silver phosphate. The precipitate was dried in 12–24 h at 50 °C in the dark. The bright yellow silver phosphate crystals were filtered and then dried at 110 °C before measuring their isotopic composition. Duplicate phosphate with known isotopic values were processed in parallel with field samples to assess the veracity of sample processing and final isotopic composition.

Around 300 μg of silver phosphate was prepared into silver capsules to measure $\delta^{18}O_P$ values using Thermo-Chemolysis Elemental Analyzer (TC/EA) coupled to a Delta V continuous-flow isotope ratio measuring mass spectrometer (IRMS; ThermoFisher Scientific, Bremen, Germany). The measured $\delta^{18}O_P$ values were calibrated against YR series standards (−5‰ and +33‰) that were originally calibrated using the conventional fluorination method.

The oxygen isotopic composition of water ($\delta^{18}O_w$) was measured from all watershed waters. For standard measurement, about 0.3 mL of water was equilibrated with CO_2 at 26.0 °C in borosilicate vials for 24 h. The isotopic composition of headspace CO_2 after equilibration was measured using a GasBench II coupled to IRMS (ThermoFisher Scientific, Bremen, Germany) and calibrated using two USGS standards (W67400 and USGS W32615 with $\delta^{18}O_w$ values of −1.97‰ and −9.25‰, respectively). Triplicate standards were analyzed with a precision of <0.10‰. A temperature-dependent equilibrium fractionation between CO_2 ($\delta^{18}O_{CO2}$) and H_2O ($\delta^{18}O_{H2O}$) (Cohn and Urey, 1938) was used to calculate $\delta^{18}O_w$ values. All oxygen isotopic values of P_i and water are reported in standard delta notation in per mil (‰) with respect to Vienna Standard Mean Ocean Water (VSMOW).

To identify the extent to which P pools in soils and colloids are biologically cycled, the equilibrium isotope composition was calculated using the temperature-dependent fractionation equation developed by Chang and Blake (2015):

$$\delta^{18}O_P = \left(\delta^{18}O_W + 10^3\right)\cdot e^{\frac{\left[\left(14.43\cdot\frac{10^3}{T}\right)-26.54\right]}{10^3}} - 10^3 \quad (1)$$

where $\delta^{18}O_P$ and $\delta^{18}O_w$ refer to oxygen isotope values of P_i and water, respectively, and T denotes the water temperature in degrees Kelvin (K).

3. Results

3.1. Salinity and chlorophyll a

The changes in salinity in seven different sites in the Love Creek in different months from March 2017 to September 2017 are shown in Fig. 2. Salinity in the non-tidal sites (GN, BN, and LN) was around 0 ppt at all times but increased steadily down in the tidal sites of the creek (LT4, LT3, LT2, and LT1) and reached the maximum (~35 ppt) at its mouth. The high salinity of LT1 indicated that water from this site is not different from that of Delaware Bay (PDE, 2012). The concentration of chlorophyll *a* was almost zero in the non-tidal section and steadily increased with salinity until salinity of 10 (±5) ppm at the middle of Love Creek (LT4) and then declined with the further increase in salinity. While the trend of chlorophyll *a* concentration was the same all months, the changes at a site followed the trend of warming temperature with the highest concentrations in June or July (Fig. 2).

3.2. P pools in colloids, soils, and plant debris

Concentrations of P_i in different P pools in colloids in three different months are shown in Fig. 3a. In general, colloidal samples collected in July have a relatively higher P_i concentration of all pools from all sites than the other two months. Interestingly, the order of concentration of P_i is the same in all sites and all three months as follows: NaOH-P_i > $NaHCO_3$-P_i > HNO_3-P_i > H_2O-P_i. Comparing among the freshwater and tidal sites, colloids in upstream freshwater sites are rich in P_i and become very low (<10 μmol/g) at high salinity sites. Like salinity, the P

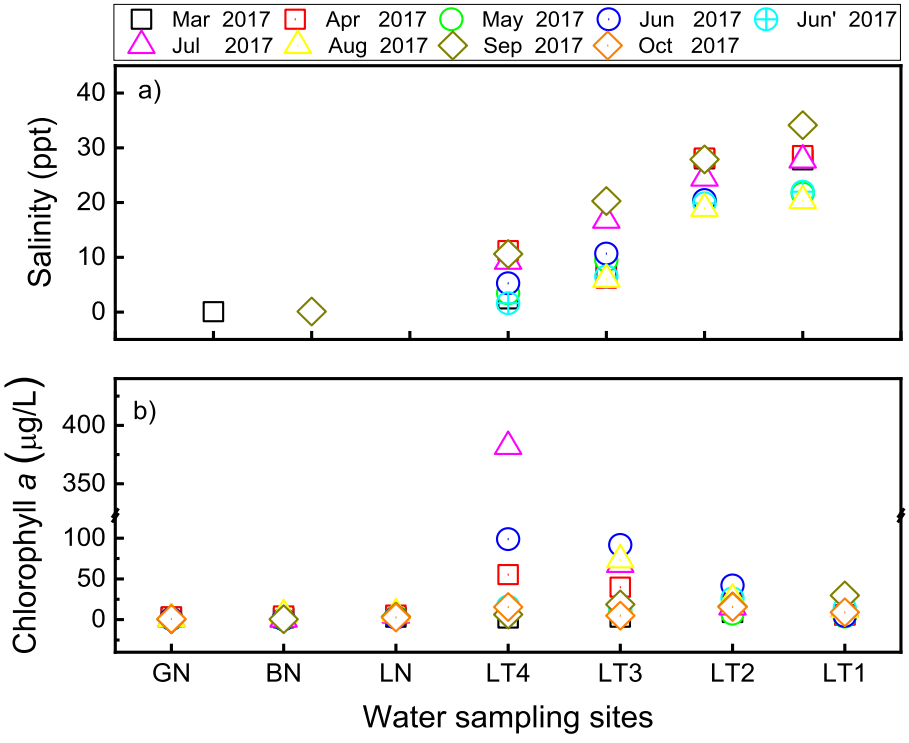

Fig. 2. Salinity (a) and chlorophyll *a* (b) concentration in waters collected from the Love Creek. The same month with apostrophe (') means two measurements made in the specific month.

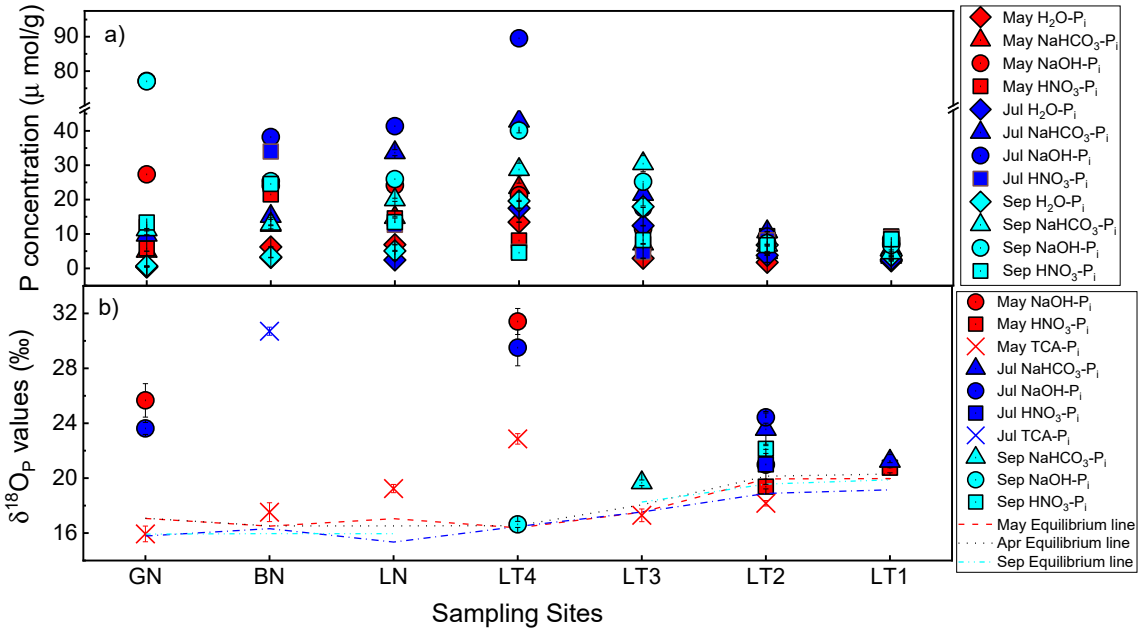

Fig. 3. a) Concentrations and b) isotopes of different P pools of colloids collected in three months in May, July, and September. The dotted lines in b) represent equilibrium isotopes in the sampling times calculated from the measured water isotopes and temp using the Eq. (1) in the text.

content in colloids at the site LT4, tidal- and non-tidal boundary site, was relatively high.

Concentrations of P_i in different P pools of three different size fractions (≥53 μm, 0.45–53 μm, and 0.10–0.45 μm) of surface soils are shown in Fig. 5. A reverse trend of concentration with soil size fraction ws observed. Soil from the smallest size fraction (0.10–0.45 μm) had the highest P_i concentration in all pools compared to the other two soil size fractions. Among different landforms, forest soils (LC6–7) had a relatively low concentration of P_i. As expected, P_i concentrations of septic tank waste were one to two orders of magnitude higher than that of soils (Fig. 5). In general, P_i concentrations in TCA-P_i of plant debris were much lower than that of colloids and generally increased along the direction of increasing salinity, while no specific pattern was observed for HNO_3-P_i in plants (Fig. SI2). Comparatively, TCA-P_i contributed around 55–70% of total P in plant debris. The ratio of NaOH-P_i to HNO_3-P_i for colloids is usually similar to that of forest soil (LC6–7) and relatively low compared to farm soils. The site at the middle of Love Creek (LT4) was anomalous as it showed an unexpectedly high ratio (similar to other parameters such as P content and chlorophyll *a*). An inverse relationship of soil particle size and the ratio of NaOH-P_i to HNO_3-P_i was observed (Fig. SI3).

3.3. Isotope composition of carbon and nitrogen and C/N ratio

From March 2017 to September 2017, $\delta^{13}C$ values of colloids enriched gradually downstream from −28.6‰, the monthly average for GN, to −21.3‰, the monthly average for LT1. Colloids in LT4 had the lightest $\delta^{13}C$ values (≈−30‰) in September 2017 compared to other sites, which may be the result of an exceptionally high concentration of chlorophyll *a* in the LT1 site (Fig. 2b). Similarly, the $\delta^{15}N$ values of colloids mirrored those of $\delta^{13}C$ values along the water flow direction. From LT4, the average colloidal $\delta^{15}N$ values steadily became lighter downstream from 9.2 to 6.5‰ in the Love Creek Watershed (LT1) (Fig. 4b). A seasonal comparison shows the variability in $\delta^{15}N$ values was relatively less than that of $\delta^{13}C$. The highest difference was observed in site BN with $\delta^{15}N$ value of 2.2‰ and 5.3‰ in July and September, respectively. The same site showed high variability in $\delta^{13}C$, with values of −27.8 in July and −17.4‰ in September 2017. Comparison of C/N ratios along the flow direction showed an analogous pattern with $\delta^{13}C$ values; specifically, the ratio steadily decreases with increasing salinity (Fig. 4c). The exceptionally low C/N value of colloids was observed at site LT4, which is caused by a high concentration of chlorophyll *a*, compared to other sites.

The $\delta^{13}C$ values of plant debris gradually enriched downstream from −31.5‰ (GN) to −19.2‰ (LT1). Similarly, $\delta^{15}N$ values of plant debris had an analogous pattern along the water flow direction with that of $\delta^{13}C$. From site BN the average $\delta^{15}N$ values of plant debris steadily enriched downstream from −4.7 to +6.0‰ at LT2 (Fig. 4e). Comparing C/N ratios along the flow direction, an opposite pattern with $\delta^{13}C$ was observed, as the ratio steadily decreased with increasing salinity (Fig. 4f). The exceptionally high C/N ratio of plant debris was observed at site LT4, which mirrors the high concentration of chlorophyll *a*.

The $\delta^{13}C$ values of two different size fractions of surface soils from farms were relatively constant with values ranging from −23‰ to −21‰, while those from forests (LC6, LC7) were distinctly lighter (*ca.* −27‰ (Fig. 7). For soils from different depths (0–10 cm and 10–20 cm), $\delta^{13}C$ values were also consistently similar (−23‰ to −21‰) (Fig. SI4). Similar patterns appeared for $\delta^{13}C$ of soils from the same farms and forests among three different size fractions (53 μm, 0.45–53 μm, and 0.10–0.45 μm) (Fig. 6a). There was no difference in $\delta^{13}C$ values between different soil size fractions irrespective of sampling depth and crop type. Similarly, $\delta^{15}N$ values of two different size fractions of all surface soils from farms were around +6‰, while those from forests (LC6 and LC7) had distinctly lighter $\delta^{15}N$ values at *ca.* +2‰ (Fig. 6b). For soils from different depths (0–10 cm and 10–20 cm), $\delta^{15}N$ values were also stable at *ca.* +6‰) (Fig. SI4). A similar pattern emerged for $\delta^{15}N$ values of soils combined from the same farms and forest with three different size fractions (≥53 μm, 0.45–53 μm, and 0.10–0.45 μm) (Fig. 6a). A comparison of C/N ratios with size fractions showed a distinct pattern in $\delta^{13}C$ and $\delta^{15}N$ values, as C/N ratios steadily increased with decreasing size fractions (Fig. SI5). Generally, no significant difference in C/N ratio was observed between forest and farm soil. A hierarchical cluster analysis of all data showed similar results (Fig. SI7).

3.4. Phosphate oxygen isotope ratios of different P pools

For NaOH-P_i, $\delta^{18}O_P$ values of two different size ranges (0.45–53 μm and 0.10–0.45 μm) of all combined soils from farms were comparable

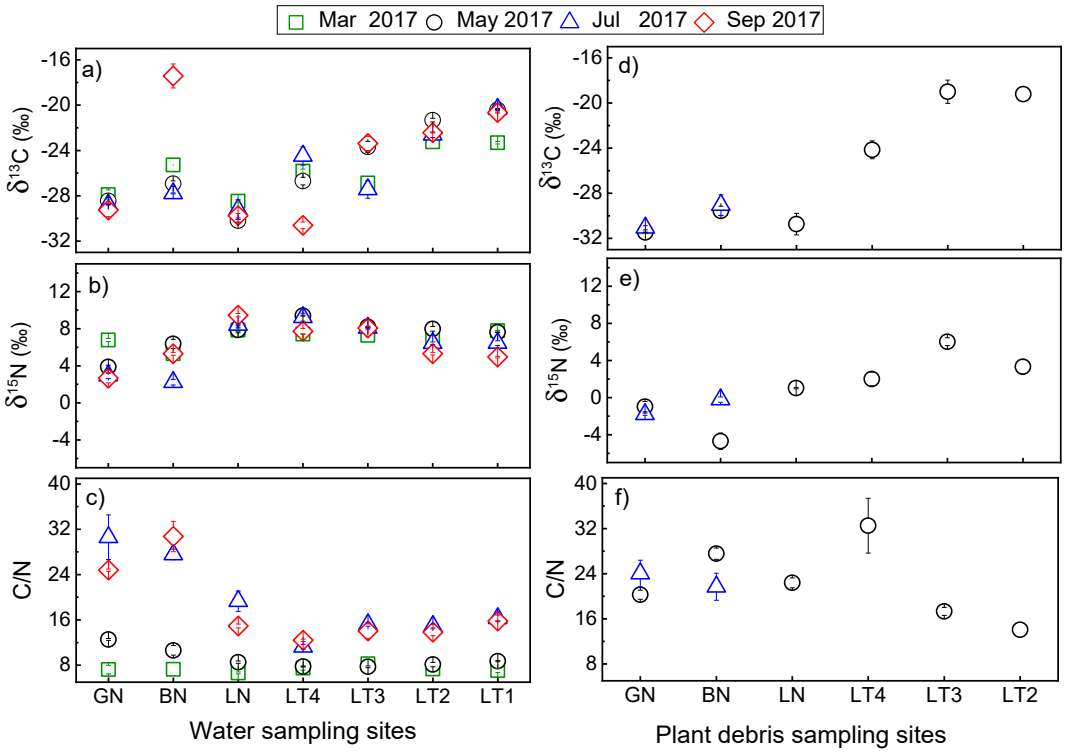

Fig. 4. a) Measured $\delta^{13}C$, b) $\delta^{15}N$, and c) C/N ratios of colloids in March, May, July and September 2017. The right panel shows d) $\delta^{13}C$, e) $\delta^{15}N$, and f) C/N ratios of plant debris in May and July 2017. GN, BN and LN are freshwater sites and LT1–4 are tidal sites.

and relatively constant with values ranging from 19‰ to 21‰ (Fig. 6c). Intriguingly, $\delta^{18}O_P$ values of larger soil fraction (≥53 μm) were distinct (*ca.* 4‰ difference). No significant difference in $\delta^{18}O_P$ values of NaOH-P_i is observed between farm soil and forest soil. For HNO_3-P_i, a similar size-related pattern was observed for $\delta^{18}O_P$ values of soils between sandy (≥53 μm) and silt fraction (0.45–53 μm) (Fig. 6d). Interestingly, $\delta^{18}O_P$ values of two different size ranges of all surface soils from farms were around +18‰, while those from the forest (LC6–7) have distinct heavier $\delta^{18}O_P$ values (*ca.* +22‰) (Fig. 6c, d).

The measured $\delta^{18}O_P$ values of different P pools of the colloids and plant debris and the theoretical equilibrium values calculated using Eq. (1) (see above) by Chang and Blake (2015) are presented in Fig. 3b. The $\delta^{18}O_P$ values for NaOH-P_i pool of colloids at GN and LT4 in May 2017 were heavier than the calculated equilibrium values by *ca.* 8.8–13‰, as was the one of NaOH-P_i pool of colloids collected at GN and LT4 in July 2017. The $\delta^{18}O_P$ values for HNO_3-P_i pools of colloids collected at two sites (LT2 and LT1) in both May 2017 and July 2017 were heavier than the calculated equilibrium values by *ca.* 2–3‰. But the isotopes of NaOH-P_i pool of colloids at LT2 site in May 2017 were slightly lighter than the calculated equilibrium values by *ca.* 0.5‰. The $\delta^{18}O_P$ values for TCA-P_i pools of plant debris were close to the equilibrium values except for sites LN (*ca.* 2‰) and LT4 (*ca.* 7‰) in May 2017, while that of BN was *ca.* 13‰ heavier than the equilibrium $\delta^{18}O_P$ values in July 2017.

3.5. Results from elemental composition based on PCA

To determine the correlation among water samples and the relative importance of different variables, PCA was used to identify two significant components ($\lambda > 1$) that collectively explained 53% of the variance in surface water with water flow. The loading plot and correlation matrix resulting from the PCA showed a wide gradient in nutrient species distribution in surface water over 8 months in the upstream and downstream stretch in the Love Creek (Fig. SI6). Total phosphorus (TP) and chlorophyll *a* in the water column were strongly correlated with each other (Group 1). Dissolved inorganic phosphate (DIP) and ammonium were located near the intersection point, which suggests that either they were not correlated at all or that they were not explained by two components used in PCA analysis. Moreover, TP and total nitrogen (TN) were orthogonal to each other, indicating that they were not related. The clear separation between N and P forms in the water column suggests that they may originate from different sources with water flow.

4. Discussion

4.1. Salinity and chlorophyll a

Primary productivity is reflected in high and very high chlorophyll *a* concentrations, suggesting oligo-mesotrophic and eutrophic conditions in the non-tidal and tidal segments of Love Creek (KDHE, 2011), respectively. The phytoplankton debris contributes to the particulate matter as well, which requires careful consideration because of their rich inorganic components. For instance, the relative content of chlorophyll *a* in phytoplankton biomass can vary. The content is reported to be 0.08% to 1.88% in shallow lakes (Vörös and Padisak, 1991) and 0.308% to 0.702% across a broad trophic gradient of oligotrophic to highly eutrophic lakes (Kasprzak et al., 2008).

Phytoplankton in LN and LT4 contributed to more than 45% of total particulate matter, while their contribution was less than 15% for other sites when the ratio between chlorophyll *a* and phytoplankton is selected arbitrarily at 1%. Please note that this calculation is based on the wet weight of phytoplankton and thus their contribution would be lower if based on their dried weight. The influence of phytoplankton on particulate matter in other sites is likely negligible, while the impact in LN and LT4 is considerable. This may also suggest an unknown nutrient source or different physicochemical processes at the tidal-non-tidal boundary site.

4.2. Variation of P in colloids, size fractions of soil, and plant debris

The ranges in colloidal P concentrations in the study sites were comparable to other estuaries in the regions such as in the mouth of East Creek (Mingus et al., 2019) and the mouth of Deer Creek-Susquehanna River (Li et al., 2019) in the Chesapeake Bay. Similarly, total P and colloid concentrations were comparable to the Patuxent estuary of the Chesapeake Bay (Jordan et al., 1997). While there could be loading-related reasons for the increase in colloidal content downstream, salt-induced aggregation of fine particles is often the primary reason.

In general, the order of the concentration of P_i in different P pools of colloids and soils was NaOH-P_i > $NaHCO_3$-P_i > HNO_3-P_i > H_2O-P_i (Figs. 3a and 5). Most obviously, NaOH-P_i, which varied from 6.8 to 77.1 μmol/g, constituted the major P sink for colloids (30.8–77.7% of total P), corresponding to P tightly bound with Fe and Al minerals (Hedley and Stewart, 1982). This restul is comparable to the P pools in the suspended particulate matter in Susquehanna River (Li et al., 2019) and East Creek (Mingus et al., 2019) and agricultural soils (Joshi et al., 2016). This similarity implies that one major source of colloids in surface waters is soil. One exception was that NaOH-P_i in GN site (July and September) contributed *ca.* 80% of total colloidal P, while NaOH-P_i in other sites contributed *ca.* 40%, indicating that the composition of colloids in GN site could be significantly different from other sites. This contribution of NaOH-P_i to total colloidal P was slightly less than that in Jordan et al. (2008) in the Patuxent estuary. This could be due to differences in salinity and separation methods (*i.e.*, visible plant debris and algae were removed before centrifugation in this study). The relatively gradual depletion of P in colloids from May to July and to September may reflect compositional differences in colloidal sources upland and in biogeochemical process that alter colloidal P speciation (Hartzell et al., 2017).

Significant differences in P concentrations of all four P pools were observed between farm (4.27–5.70 μmol/g) and forest (10.99–31.42 μmol/g) soils (Fig. 5). The continuous fertilization in farm soil builds up the legacy P and results in higher P content. With decreasing size fraction, P content increased in both farm and forest soils. The P concentration in the smallest soil size fraction (0.10–0.45 μm) was *ca.* 50% higher than that of the larger fractions (≥53 μm) (Fig. 5), which may have resulted from the difference in mineral compositions among differing soil size fractions. Specifically, finer particles that have the high specific surface area and P content and are prone to mobilization during runoff, thus may disproportionately contribute high to total colloidal mass. In contrast, larger colloids with low P content are only mobilized in high-intensity precipitation-driven floods (Sharpley et al., 1998).

Concentrations of P_i in septic tank wastes were one or two orders of magnitude higher than that of soils and with slightly different order of the concentration of P pools: HNO_3-P_i > $NaHCO_3$-P_i > NaOH-P_i > H_2O-P_i (Fig. 5). It is intuitive to expect the HNO_3 pool, which corresponds to P tightly bound to Ca minerals (Hedley and Stewart, 1982), should be dominated in colloidal P if the septic sources of P are considerable in the water column. This, however, was not the case in colloids (Fig. 3a). The $NaHCO_3$ pool in septic waste was high (*ca.* 124 μmol/g), which suggests that the large portion of colloidal P derived from the septic wastes should be readily bioavailable to microorganisms. Note that the location of the septic waste sampling site was near water sampling site LT4, which has outliers in different parameters. Therefore the specific contribution of different sources requires additional high-resolution studies.

Based on the P mass balance, TCA-P_i contributes 55–70% of P in plant debris indicating that the large portion of P in plant debris was bioavailable to microorganisms. A slight revision was made to the extraction method for plant debris in this study that 10 M HNO_3 was used to extract structural P in the residual plant debris after TCA extraction. In general, P_i concentrations in TCA and HNO_3 pools were lower than in a past plant study (Pfahler et al., 2013). This difference could be due to the processing-related factor, such as plant debris in this study was composited and dried, while Pfahler et al. (2013) used fresh leaves. Furthermore, there was a difference in the size of P pools along the salinity gradient: concentrations TCA-P_i generally increased with increasing

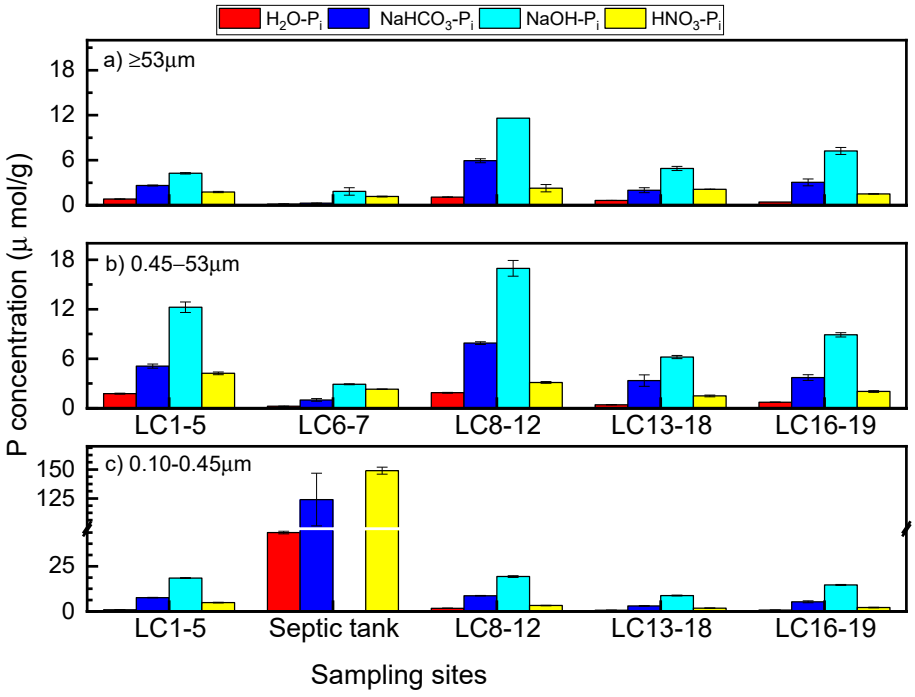

Fig. 5. Concentrations of P_i pools of different size soil fractions: a) ≥53 um, b) 0.45–53 μm, and c) 0.10–0.45 μm. Due to the small total mass of all soil from LC6–7, only two size fractions are shown. Please note septic tank samples were not separated into different size fractions.

salinity, while no clear pattern was present in HNO_3-P_i. A direct comparison in P pools between plant debris and colloids can be made but is inaccurate because different extraction methods were employed. However, high concentrations of Fe and Al in plant debris extracts aid in explaining the discrepancy in the unexpectedly high contribution of NaOH-P_i to total colloidal P in GN site in July and September.

4.3. Isotope composition of carbon and nitrogen and C/N ratio

Both $\delta^{13}C$ and $\delta^{15}N$ values of forest and farm soils are different, similar to those reported before (Awiti et al., 2008). In general, $\delta^{13}C$ values in farm soils were more enriched compared to forest soils. This is most likely resulted from the yearly crop rotation of C4 plants (maize) with C3 plants (soybean), with average $\delta^{13}C$ values of −12.7 and −29.6‰, respectively (Lamb et al., 2006; Smith and Epstein, 1971). Similar $\delta^{15}N$ enrichment in farm soils than forest soil may result from relatively closed N cycle in natural forests and selective loss (Eshetu, 2004). Because of the preferential uptake of lighter N isotopes by microorganisms during soil biogeochemical processes such as mineralization and nitrification, losses of soil nitrogen following cultivation could result in heavier $\delta^{15}N$ signatures in soils (Högberg, 1997; Awiti et al., 2008). No significant differences in isotope values of C and N were observed among different soil size fractions irrespective of sampling depth and crop/forest type in farm and forest soils. It is unclear the reason for the similarity but the identical trend observed in the past has been interpreted to be due to redistribution of nutrients (Djodjic et al., 2004). Nonetheless, the similarity of isotope values benefitted source tracking of colloidal P.

The $\delta^{13}C$ values of plant debris had an analogous pattern to that of colloids across the salinity gradient and varied within a similar isotopic range (Fig. 4a, d). For example, the $\delta^{13}C$ values of colloids (−30‰ to −26‰) in freshwater sites (GN, BN, and LN) were *ca.* −6‰ lighter than the ones of different size fractions of farm soils, indicating that plant debris (−32‰ to −29‰) is the major colloidal source in upstream of the Love Creek (Fig. 4a). The $\delta^{13}C$ values of C3 plants (≈−32 to −21‰) were isotopically depleted compared to those of C4 plants (≈−17 to −9‰) (Lamb et al., 2006; Smith and Epstein, 1971). For aquatic plants such as phytoplankton, $\delta^{13}C$ values were between −42 and −24‰ with an average of −30‰ (Hamilton and Lewis, 1992; Kendall et al., 2001). Similarly, C/N ratios of autochthonous sources such as plankton are low (5–8) (Li et al., 2016) compared to land-derived vascular plants (>15) (Meyers, 1994; Savoye et al., 2003) while that of soil organic matter lie in the intermediate range (8–15) (Brady and Weil, 1990). The low concentration of chlorophyll *a* (less than 1 μg/L in May and July; Fig. 2b) rules out the possibility that phytoplankton may have been an important source that would decrease the $\delta^{13}C$ values of colloids. The $\delta^{15}N$ values of colloids in the freshwater sites (GN and BN) were significantly lighter than that of the tidal zone (LT2 and LT1). Similarly, the C/N ratios of colloids in the freshwater sites were quite similar to that of plant debris (Fig. 4f) and decreased sharply before becoming almost steady with salinity gradient. This further confirmed that the major source of colloids upstream was plant debris, whose $\delta^{15}N$ values and C/N ratios are much lower than that of farm soils and heavier than those of septic tanks (Figs. 6 and SI5). Forest soils could be one of the major sources of colloids because of their low C/N ratios in May 2017 (*ca.* 12), while the relatively high C/N ratio of colloids precludes the potential of forest soils as the major source of colloids in July 2017. This may indicate variability in the proportion of different sources of colloids in upstream of the Love Creek. Some outliers, such as the $\delta^{13}C$ values of colloids in BN and LT4 sites in September, could potentially be explained by seasonal variation of different sources or switching of tree leaves to corn debris under certain conditions. In essence, the colloids of upstream Love Creek were dominated by non-agricultural sources.

In contrast to the general trend in estuarine environments, $\delta^{13}C$ values of colloids enriched gradually downstream from −28.6‰ to −21.3‰, implying variability in the proportion of different sources or switching of the major source along the salinity gradient. For example, colloids in LT4 site had intermediate $\delta^{13}C$ (≈−26.91‰) and $\delta^{15}N$ (+8.50‰) values as compared to that of forest soils ($\delta^{13}C$: −27.80‰; $\delta^{15}N$: +2.00‰), farm soils ($\delta^{13}C$: −22.00‰; $\delta^{15}N$: +5.00–8.60‰) and plant debris ($\delta^{13}C$: −24.00‰; $\delta^{15}N$: +2.00‰). These results confirm that the contribution of plant debris decreased downstream. Meanwhile, the low C/N ratios of colloids (9.7) reduced the possibility that plant debris (32.5) served as a major source of colloids in LT4 site. Moreover, as discussed in Section 4.1, phytoplankton in LT4 site contributed more than 45% of total particulate matter and is the major source of colloids. Furthermore, colloids in LT2 site had similar $\delta^{13}C$ (≈−21.4‰) and $\delta^{15}N$ (+6.7‰) values to those of farm soils (*ca.* 3‰ different from plant debris), proving that the major source of colloids in the creek water switched from plant debris upstream to phytoplankton and farm soils downstream. Septic tanks ($\delta^{13}C$: −24.35‰; $\delta^{15}N$: +2.0‰) and sediments may also contribute to colloids with temporal and spatial variability. However, any contribution of these two sources requires further validation through high-resolution studies or related modeling.

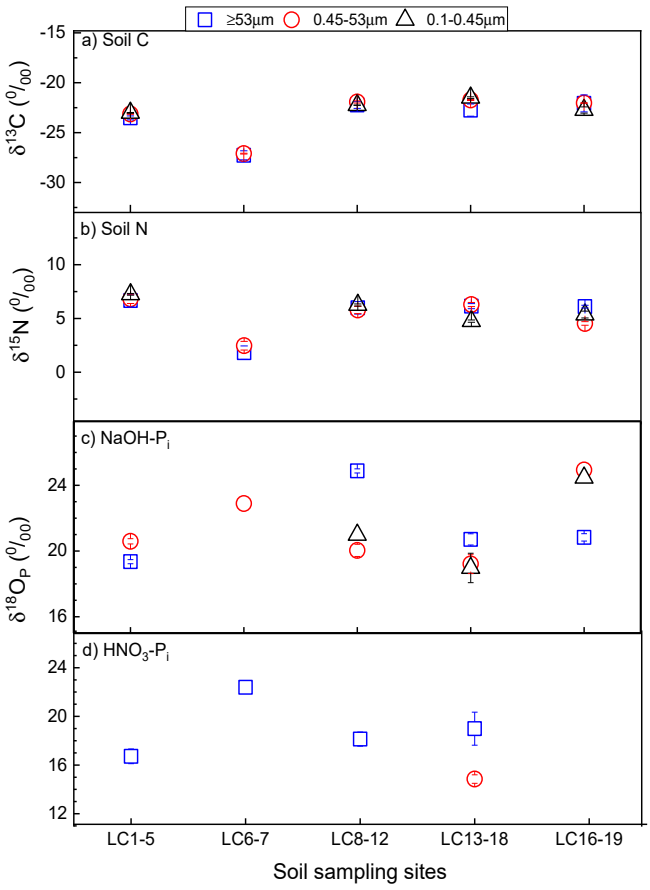

Fig. 6. Measured isotope values of a) soil carbon ($\delta^{13}C$), b) soil nitrogen ($\delta^{15}N$), c) soil NaOH-P pool, and d) soil HNO_3-P pool of surface soils.

4.4. Phosphate oxygen isotopes of different P pools

Comparision of measured isotopes colloidal P to equilibrium isotope at the time of sampling and the zone that covers a month of variability in temperature and water isotopes show that the majority of the data are out of equilibrium (Fig. 3). Among P pools, isotope values for NaOH-P_i and HNO_3-P_i pools in colloids were distinctly heavier, which implied that their isotopes may be suitable for identifying sources (Bi et al., 2018; Joshi et al., 2016; Mingus et al., 2019). The $\delta^{18}O_P$ values of TCA-P_i of plant debris and $NaHCO_3$-P_i pools at LT3 and LT1 sites were located

within the calculated equilibrium range, which indicated that these P pools were microbially cycled (Gross and Angert, 2015; Tamburini et al., 2012; Tonderski et al., 2017). Intriguingly, the $\delta^{18}O_P$ values of NaOH-P_i pool at LT4 site (September 2017) were also close to the equilibrium value and the reason for this outlier was not clear.

For the same NaOH-P_i pool, $\delta^{18}O_P$ values of silty (0.45–53 μm) and clay (0.10–0.45 μm) fractions of soils were found to be *ca.* 4‰ enriched or depleted with the ones of sandy fraction (≥53 μm). A similar pattern was found in HNO_3-P_i pools of silty (0.45–53 μm) and sandy (≥53 μm) fractions. To our knowledge, this is the first report of $\delta^{18}O_P$ values of two recalcitrant P pools in soil fractions across different size ranges, both of which lies within a narrow range: 18.97–24.88‰ and 14.85–18.99‰, respectively. The $\delta^{18}O_P$ values of both NaOH-P_i pool and HNO_3-P_i pools are comparable to similar research in soils (Bi et al., 2018; Granger et al., 2017; Hacker et al., 2019; Joshi et al., 2016; Mingus et al., 2019). The possible reasons for the minor difference could be due to different mineralogy and potential P sources or forms in these P pools, originally distinct isotopes or different contributions of microbially cycled P (Angert et al., 2012; Bauke et al., 2018; Bi et al., 2018). SEM analyses of different size fractions revealed compositionally distinct biological and abiotic components (data not shown). The difference in P content between small size soil fractions than that in larger size fraction of soils is consistent with this notion (*see* Section 4.2). Despite some uncertainties, this distinct variation in $\delta^{18}O_P$ values of different soil fractions may provide an opportunity for identifying grain-size specific P sources. For example, for precise comparison, $\delta^{18}O_P$ values of the same P pools and size range from land-derived sources and colloids are needed. This is because bulk isotope is the mixture of signatures from different size fractions. A significant difference (4–10‰) in $\delta^{18}O_P$ values of NaOH-P_i pool between silty and clay fractions of soil and colloids indicated that farm soil is less likely a major contributor for colloids in freshwater sites of Love Creek.

The $\delta^{18}O_P$ values of TCA-P_i of most plant debris were within the calculated equilibrium range (Fig. 3), which suggests that this P pool was microbially cycled. Outliers were also observed in BN and LT4 site with $\delta^{18}O_P$ values 8‰ and 13‰ higher than the equilibrium but are comparable to that of colloids in freshwater sites. Moreover, significant variation in $\delta^{18}O_P$ values in BN site from May to July and comparable changes in sink sites suggest major contribution by plant debris source of P.

4.5. Sources of colloids and associated P in water

Colloidal P encompasses solid phase of P derived from land sources as well as *in-situ* production. Colloidal P can be partly bioavailable at different temporal scales because it includes readily bioavailable P pools among other non-bioavailable P pools (Mingus et al., 2019). The extent of bioavailability depends on the composition of the different P pools, and ambient physical and chemical processes, residence time, and microbial community structure and activity. The significant overlap of C and N isotopes and C/N ratios between plant debris and colloids in upstream stretch of the creek (Fig. 8) strongly suggests that plant debris was a major source of colloids in the upstream Love Creek. These sources could be plant debris, such as leaves and partially degraded litters, whose P_i can be released into water column during transport and degradation (Cowen and Lee, 1973; Zhang et al., 2017). This result is uncommon and different from other comparable and agriculture-rich watershed such as from Gooddy et al. (2016) and Mingus et al. (2019), in which main P loading is derived from agricultural sources in the watershed. However, each watershed has unique features and drivers of nutrient loading and transport. At the least, results from Love Creek watershed points that results may not generalized among watersheds.

The lower (tidal) portion of the watershed has different sources compared to its non-tidal stretch. The similarity in independent parameters, sizes of P pools and C and N isotopes, between farm soils and colloids in tidal portion of watershed indicates that the farm soils could be the major source of colloids for tidal portion of Love Creek, which are explained below. The isotope and mass correlation of C and N clearly shows two clusters, with a distinct group for freshwater and tidal portion of the creek (Fig. 8). The P load contribution from agricultural fields is normally expected to be higher than other soils due to the loose soils which is prone to soil erosion and high P content in crop soils. For example, P concentration of different P pools in farm soil was uniformly much

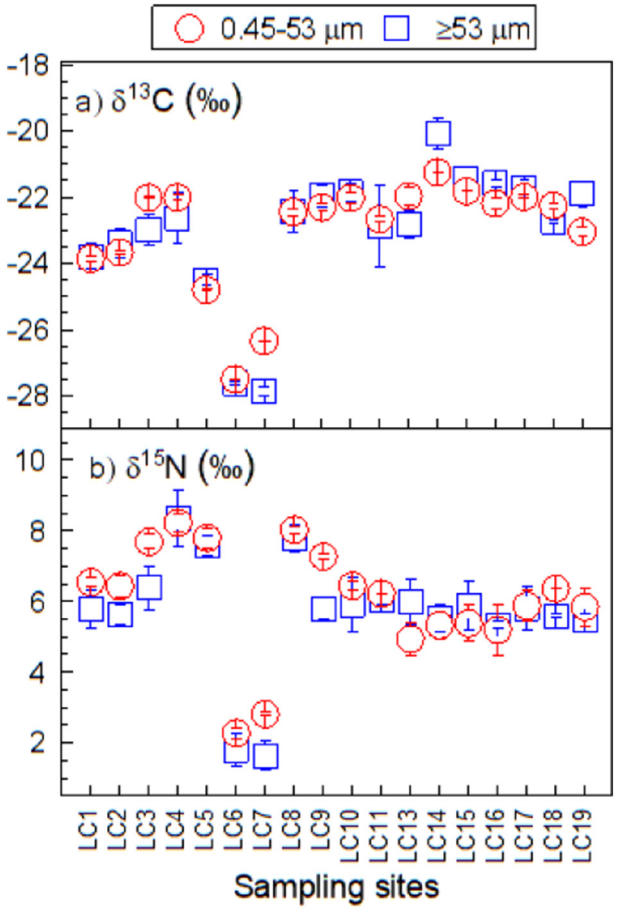

Fig. 7. Measured $\delta^{13}C$ (a) $\delta^{15}N$ (b) istopes of soils in two different size fractions of surface soils. Here isotopes of three different size fractions of combined for all soils.

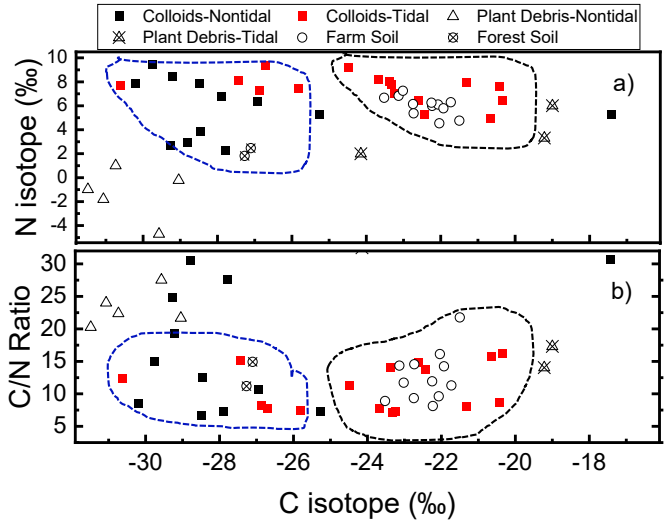

Fig. 8. Comparison of $\delta^{13}C$-$\delta^{15}N$ values (a) and $\delta^{13}C$-C/N ratios (b) of soils from different sources and that of colloids.

higher than forest soils, irrespective of size fractions (Figs. 3a, 5) but similar to that of colloidal P in the tidal stretch. Moreover, the ratio of NaOH-P_i to HNO_3-P_i pools of colloids and farm soil was similar in all sites. The site LT4 is distinct in hydrological connection-being next to undergoing major land development and water impoundment. This site always showed an anomalously high chlorophyll *a* concentration. The presence of algae debris in the particulate matter also contributed to P pool. A close relationship of chlorophyll *a* and TP in PCA analyses (Fig. SI6) indicates that phytoplankton contributes to the colloidal composition, which gradually decreases to other sites (*e.g.*, LN site). In the hierarchical cluster analysis (Fig. SI7), colloids in freshwater sites (GN, BN, and LN) were grouped with plant debris and forest soil, indicating the major sources of upstream Love Creek are non-agricultural sources. Similarly, colloids in the tidal portion (LT3, LT2, and LT1) were grouped with farm soil, confirming the major shift from non-agricultural sources into agricultural sources of P in the creek.

Comparison of P pools among sources and sinks can provide some insights on potential sources. NaOH-P_i and HNO_3-P_i pools are generally considered to be recalcitrant and may carry original P source signatures (Mingus et al., 2019; Li et al., 2019), implying that microbial cycling could be very limited due to the presence of other readily available pools for nutritional needs and geochemical processes in the site do not form these pools. In that case, they are suitable for source tracking. NaOH-P_i $\delta^{18}O_P$ values of silty and clayey fractions of soil differed by 4–10‰ from that of colloids (Figs. 3b and 6c), which suggests that the agricultural soils are the least likely sources of P. To the contrary, similarities in NaOH-P_i $\delta^{18}O_P$ values were observed between farm soils and colloids in LT2, suggesting the potential agricultural P sources for the tidal section of Love Creek.

A gradual decrease in the ratio of NaOH-P_i to HNO_3-P_i in colloidal P occurred from upstream (2–4) to downstream (0.95) (Fig. SI3). This trend is expected along the salinity gradient where physicochemical processes such as source mixing, partial removal, or formation of specific P pools occurs along an increasing salinity (Jordan et al., 2008; Mingus et al., 2019). One of the major reasons for this trend is the release of Fe-oxide bound P and consequent removal as Ca-P precipitation induced by high concentrations of Ca and high pH at high salinity (Li et al., 2017). The proportion of HNO_3-P_i (Ca-P mineral pool) increases gradually from the non-tidal to tidal portion of Love Creek. The dilution of terrestrially derived colloids upstream by importing colloids from river mouth during incoming tide may also have played a role in the depletion of NaOH-P_i/HNO_3-P_i ratio. This could be a reason for the discrepancy of the NaOH-P_i/HNO_3-P_i ratio between colloids in the tidal section and farm soils. Processes involving the formation and removal of colloids in waters are more complex. For example, a significant portion of particulate matter was derived from coastal water in a coastal estuary due to the flocculation caused by increased salinity (Mingus et al., 2019). Collectively, our different and independent data sets that include P pools and isotopes of C, N, and phosphate pointed out that two different sources dominate the colloidal P in the non-tidal and tidal portion of the creek.

5. Summary and conclusions

Concentrations of inorganic P (P_i) pools in colloids along the salinity gradient vary in the order NaOH-P_i > $NaHCO_3$-P_i > HNO_3-P_i > H_2O-P_i. The NaOH-P_i is the most dominant P pool in all colloids and soils analyzed in this study. The relative size of P pools in different size fractions in farm and forest soils are comparable but the P_i concentration of each P pool was much higher in agricultural soils. Comparison based on the C and N isotopes, concentration, and phosphate oxygen isotope of P pools suggested that the major source of colloidal P in the non-tidal section of Love Creek is non-agricultural sources such as plant debris from forest sources, but in tidal section, agricultural soils dominate. Along the salinity gradient, the contribution of terrestrial sources gradually decreased. These results collectively suggest that multiple stable isotopes provide complementary information to identify the relative contribution of colloidal P from different land uses and landforms in a water body.

CRediT authorship contribution statement

Qiang Li: Conceptualized the project, collected samples, processed and analyzed date and composed the manuscript.

Hezhong Yuan: help collect sample and partial processing and data generation, revised/revised the manuscript.

Hui Li: help collect sample and partial processing and data generation, reviewed/revised the manuscript.

Christopher Main: generated partial data, reviewed/revised the manuscript.

Jessica Anton: Effort on sample collection and partial processing and data generation.

Deb P. Jaisi: Conceived the grant and conceptualized the project.

Declaration of competing interest

The authors declare no conflict of interest.

Acknowledgments

This research was funded by NSF grants (1654642 and 1757353) and University Doctoral Fellowship. QL would like to thank Baoshan Chen and Zhaohua Jiang for the help on preparing the sitemap.

Appendix A. Supplementary data

Supplementary data to this article can be found online at https://doi.org/10.1016/j.scitotenv.2021.148353.

References

Angert, A., Weiner, T., Mazeh, S., Sternberg, M., 2012. Soil phosphate stable oxygen isotopes across rainfall and bedrock gradients. Environ. Sci. Technol. 46 (4), 2156–2162.

Awiti, A.O., Walsh, M.G., Kinyamario, J., 2008. Dynamics of topsoil carbon and nitrogen along a tropical forest–cropland chronosequence: evidence from stable isotope analysis and spectroscopy. Agric. Ecosyst. Environ. 127 (3–4), 265–272.

Bauke, S.L., von Sperber, C., Tamburini, F., Gocke, F.I., Honermeier, G.B., Schweitzer, K., Baumecker, M., Don, A., Sandhage-Hofmann, A., Amelung, W., 2018. Subsoil phosphorus is affected by fertilization regime in long-term agricultural experimental trials. Eur. J. Soil Sci. 69, 103–112.

Bi, Q.-F., Zheng, B.-X., Lin, X.-Y., Lia, K.-J., Liu, X.-P., Hao, X.-L., Zhang, H., Zhang, Z.-B., Jaisi, D.P., Zhu, Y.-G., 2018. The microbial cycling of phosphorus on long-term fertilized soil: Insights from phosphate oxygen isotope ratios. Chem. Geol. 483, 56–64.

Brady, N., Weil, R., 1990. The Nature and Properties of Soils. Macmillan, New York (ISBN 0-02-946159-6).

Chang, S.J., Blake, R.E., 2015. Precise calibration of equilibrium oxygen isotope fractionations between dissolved phosphate and water from 3 to 37 °C. Geochim. Cosmochim. Acta 150, 314–329.

Cohn, M., Urey, H.C., 1938. Oxygen isotope exchange reactions of organic compounds and water. J. Am. Chem. Soc. 60, 679–682.

Cowen, W.F., Lee, G.F., 1973. Leaves as a source of phosphorus. Environ. Sci. Technol. 7 (9), 853–854.

Davies, C.L., Surridge, B.W.J., Gooddy, D.C., 2014. Phosphate oxygen isotopes within aquatic ecosystems: global data synthesis and future research priorities. Sci. Total Environ. 496, 563–575.

DCIB, 2018. Delaware Center for the Inland Bays. www.inlandbays.org.

Desjardins, T., Andreux, F., Volkoff, B., Cerri, C.C., 1994. Organic carbon and ^{13}C contents in soils and soil size-fractions, and their changes due to deforestation and pasture installation in eastern Amazonia. Geoderma 61 (1–2), 103–118.

Djodjic, F., Börling, K., Bergström, L., 2004. Phosphorus leaching in relation to soil type and soil phosphorus content. J. Environ. Qual. 33 (2), 678–684.

Eshetu, Z., 2004. Natural ^{15}N abundance in soils under young-growth forests in Ethiopia. For. Ecol. Manag. 187 (2-3), 139–147.

Gooddy, D.C., Lapworth, D.J., Bennett, S.A., Heaton, T.H., Williams, P.J., Surridge, B.W., 2016. A multi-stable isotope framework to understand eutrophication in aquatic ecosystems. Water Res. 88, 623–633.

Granger, S.J., Heaton, T.H., Pfahler, V., Blackwell, M.S., Yuan, H., Collins, C.A., 2017. The oxygen isotopic composition of phosphate in river water and its potential sources in the Upper River Taw catchment, UK. Sci. Total Environ. 574, 680–690.

Gross, A., Angert, A., 2015. What processes control the oxygen isotopes of soil bioavailable phosphate? Geochim. Cosmochim. Acta 159, 100–111.

Hacker, N., Wilcke, W., Oelmann, Y., 2019. The oxygen isotope composition of bioavailable phosphate in soil reflects the oxygen isotope composition in soil water driven by plant diversity effects on evaporation. Geochim. Cosmochim. Acta 248, 387–399.
Hamilton, S.K., Lewis Jr., W.M., 1992. Stable carbon and nitrogen isotopes in algae and detritus from the Orinoco River floodplain, Venezuela. Geochim. Cosmochim. Acta 56 (12), 4237–4246.
Hartzell, J.L., Jordan, T.E., Cornwell, J.C., 2017. Phosphorus sequestration in sediments along salinity gradients of Chesapeake Bay subestuaries. Estuar. Coast. https://doi.org/10.1007/s12237-017-0233-2.
Hawkins, B., Polglase, P.J., 2000. Foliar concentrations and resorption of nitrogen and phosphorus in 15 species of eucalypts grown under non-limited water and nutrient availability. Aust. J. Bot. 48 (5), 597–602.
Hedley, M., Stewart, J., 1982. Method to measure microbial phosphate in soils. Soil Biol. Biochem. 14 (4), 377–385.
Högberg, P., 1997. Tansley review no. 95 ^{15}N natural abundance in soil–plant systems. New Phytol. 137 (2), 179–203.
Jordan, T.E., Correll, D.L., Weller, D.E., 1997. Nonpoint source discharges of nutrients from piedmont watersheds of Chesapeake Bay. J. Am. Water Resour. Assoc. 33 (3), 631–645.
Jordan, T.E., Cornwell, J.C., Boynton, W.R., Anderson, J.T., 2008. Changes in phosphorus biogeochemistry along an estuarine salinity gradient: the iron conveyer belt. Limnol. Oceanogr. 53 (1), 172–184.
Joshi, S.R., Li, X., Jaisi, D.P., 2016. Transformation of phosphorus pools in an agricultural soil: an application of oxygen-18 labeling in phosphate. Soil Sci. Soc. Am. J. 80 (1), 69–78.
Joshi, S., Li, W., Bowden, M., Jaisi, D.P., 2018. Sources and pathways of formation of recalcitrant and residual phosphorus in an agricultural soil. Soil Syst. 2 (3), 45.
Karl, D.M., Tien, G., 1992. MAGIC: a sensitive and precise method for measuring dissolved phosphorus in aquatic environments. Limnol. Oceanogr. 37 (1), 105–116.
Kasprzak, P., Padisák, J., Koschel, R., Krienitz, L., Gervais, F., 2008. Chlorophyll a concentration across a trophic gradient of lakes: an estimator of phytoplankton biomass? Limnologica 38 (3–4), 327–338.
KDHE (Kansas Department of Health and Environment), 2011. Water Quality Standards White Paper: Chlorophyll a Criteria for Public Water Supply Lakes or Reservoirs.
Kendall, C., Silva, S.R., Kelly, V.J., 2001. Carbon and nitrogen isotopic compositions of particulate organic matter in four large river systems across the United States. Hydrol. Process. 15 (7), 1301–1346.
Lamb, A.L., Wilson, G.P., Leng, M.J., 2006. A review of coastal palaeoclimate and relative sea-level reconstructions using δ^{13}C and C/N ratios in organic material. Earth Sci. Rev. 75 (1–4), 29–57.
Li, Y., Zhang, H., Tu, C., Fu, C., Xue, Y., Luo, Y., 2016. Sources and fate of organic carbon and nitrogen from land to ocean: identified by coupling stable isotopes with C/N ratio. Estuar. Coast. Shelf Sci. 181, 114–122.
Li, J., Reardon, P., McKinley, J.P., Joshi, S.R., Bai, Y., Bear, K., Jaisi, D.P., 2017. Water column particulate matter: a key contributor to phosphorus regeneration in a coastal eutrophic environment, the Chesapeake Bay. J. Geophys. Res. 122 (4), 737–752.
Li, Q., Yuan, H., Li, H., Wang, D., Jin, Y., Jaisi, D.P., 2019. Loading and bioavailability of colloidal phosphorus in the estuarine gradient of the deer creek-susquehanna river transect in the Chesapeake Bay. J. Geophys. Res. 124 (12), 3717–3726.
Main, C.R., Tyler, R., Lopez, K., Heurta, H., 2020. Microbial source tracking in the Love Creek Watershed, Delaware (USA). Delaware J. Publ. Health https://doi.org/10.32481/djph.2021.01.006.
McDonnell, J.J., McGuire, K., Aggarwal, P., Beven, K.J., Biondi, D., Destouni, G., Dunn, S., James, A., Kirchner, J., Kraft, P., 2010. How old is streamwater? Open questions in catchment transit time conceptualization, modelling and analysis. Hydrol. Process. 24, 1745–1754.
Meyers, P.A., 1994. Preservation of elemental and isotopic source identification of sedimentary organic matter. Chem. Geol. 114 (3–4), 289–302.
Mingus, K.A., Liang, X., Massoudieh, A., Jaisi, D.P., 2019. Stable isotopes and Bayesian modeling methods of tracking sources and differentiating bioavailable and recalcitrant phosphorus pools in suspended particulate matter. Environ. Sci. Technol. 53 (1), 69–76.
Murphy, J., Riley, J.P., 1962. A modified single solution method for the determination of phosphate in natural waters. Anal. Chim. Acta 27, 31–36.
National Eutrophication Survey Methods, 1973–1976. Working Paper No. 175.
Partnership for the Delaware Estuary, 2012. Technical Report for the Delaware Estuary and Basin. PDE Report No. 12-01. 255 pages. Available at:. https://www.nrc.gov/docs/ML1434/ML14345A530.pdf.
Pfahler, V., Dürr-Auster, T., Tamburini, F., Bernasconi S, M., Frossard, E., 2013. ^{18}O enrichment in phosphorus pools extracted from soybean leaves. New Phytol. 137 (2), 179–203 (197(1), 186–193).
Savoye, N., Aminot, A., Trégue, P., Fontugne, M., Naulet, M., Kérouel, R., 2003. Dynamics of particulate organic matter δ^{15}N and δ^{13}C during spring phytoplankton blooms in a macrotidal ecosystem (Bay of Seine, France). Mar. Ecol. Prog. Ser. 255, 27–41.
Sharpley, A., Meisinger, J., Breeuwsma, A., Sims, J., Daniel, T., Schepers, J., 1998. Impacts of animal manure management on ground and surface water quality. Animal Waste Utilization: Effective Use of Manure as a Soil Resource, pp. 173–242.
Sharpley, A.N., Bergström, L., Aronsson, H., Bechmann, M., Bolster, C.H., Börling, K., Djodjic, F., Jarvie, H., Schoumans, O.F., Stamm, C., Tonderski, K.S., Ulen, B., Uusitalo, R., Withers, P.J.A., 2015. Future agriculture with minimized phosphorus losses to waters: research needs and direction. Ambio 44, 163–179.
Siebers, N., Bauke, S.L., Tamburini, F., Amelung, W., 2018. Short-term impacts of forest clear-cut on P accessibility in soil micro-aggregates: an oxygen isotope study. Geoderma 315, 59–64.
Smith, B.N., Epstein, S., 1971. Two categories of ^{13}C/^{12}C ratios for higher plants. Plant Physiol. 47 (3), 380–384.
Tamburini, F., Pfahler, V., Bünemann, E.K., Guelland, K., Bernasconi, S.M., Frossard, E., 2012. Oxygen isotopes unravel the role of microorganisms in phosphate cycling in soils. Environ. Sci. Technol. 46 (11), 5956–5962.
Tonderski, K., Andersson, L., Lindström, G., Cyr, R., Schönberg, R., Taubald, H., 2017. Assessing the use of $\delta^{18}O_P$ in phosphate as a tracer for catchment phosphorus sources. Sci. Total Environ. 607, 1–10.
Vörös, L., Padisak, J., 1991. Phytoplankton biomass and chlorophyll-a in some shallow lakes in Central Europe. Hydrobiologia 215 (2), 111–119.
Zhang, W., Zhu, X., Jin, X., Meng, X., Tang, W., Shan, B., 2017. Evidence for organic phosphorus activation and transformation at the sediment-water interface during plant debris decomposition. Sci. Total Environ. 583, 458–465.